

Berry phases of vison transport in \mathbb{Z}_2 topologically ordered states from exact fermion-flux lattice dualities

Chuan Chen ^{1,2} Peng Rao ² and Inti Sodemann ^{2,3,*}

¹*Institute for Advanced Study, Tsinghua University, 100084 Beijing, China*

²*Max-Planck Institute for the Physics of Complex Systems, 01187 Dresden, Germany*

³*Institut für Theoretische Physik, Universität Leipzig, 04103 Leipzig, Germany*

 (Received 3 February 2022; revised 3 August 2022; accepted 19 September 2022; published 4 October 2022)

We develop an exact map of all states and operators from two-dimensional lattices of spins-1/2 into lattices of fermions and bosons with mutual semionic statistical interaction that goes beyond previous dualities of \mathbb{Z}_2 lattice gauge theories because it does not rely on imposing local conservation laws and captures the motion of “charges” and “fluxes” on equal footing. This map allows to explicitly compute the Berry phases for the transport of fluxes in a large class of symmetry-enriched topologically ordered states with emergent \mathbb{Z}_2 gauge fields that includes chiral, nonchiral, Abelian or non-Abelian, that can be perturbatively connected to models where the visons are static and the emergent fermionic spinons have a noninteracting dispersion. The numerical complexity of computing such vison phases reduces, therefore, to computing overlaps of ground states of free-fermion Hamiltonians. Among other results, we establish numerically the conditions under which the Majorana-carrying flux excitation in Ising-topologically ordered states enriched by translations acquires the 0 or π phase when moving around a single plaquette.

DOI: [10.1103/PhysRevResearch.4.043003](https://doi.org/10.1103/PhysRevResearch.4.043003)

I. INTRODUCTION

One of the best understood families of spin liquids are those featuring emergent \mathbb{Z}_2 gauge fields [1,2]. These spin liquids, which include the original Anderson short-ranged resonating valence bond state [3,4], feature a nonlocal fermion (spinon) and a “ π -flux” (vison) excitation [5–8]. Kitaev’s toric code (TC) [9] is perhaps the simplest exactly solvable model for these kind of spin liquids. A recent series of works [10–12] have shown that, beyond being an exactly solvable model, the TC offers a new way to organize the Hilbert space. In Ref. [10], it has been shown that by imposing a new type of local \mathbb{Z}_2 constraint (local symmetry) on a spin model, the local gauge invariant spin operators can be exactly mapped onto local fermion bilinears. This construction can be viewed as a generalization of the procedure that allows to solve the Kitaev honeycomb model exactly [13], where the \mathbb{Z}_2 constraint immobilizes the flux excitations leaving the fermions as the only dynamical objects of the problem. For related constructions see Refs. [13–18]. The construction of Ref. [10] provides a local map from fermion bilinear operators onto spin operators in two dimensions (2D), and it serves to rewrite in an exact manner any imaginable local Hamiltonian

of fermions as a local Hamiltonian of spins restricted to a subspace satisfying the \mathbb{Z}_2 local conservation laws. Thus, for example, any free fermion model can be obtained as an exact description of a subspace of the Hamiltonian of a spin model.

In this paper we extend the mapping of Ref. [10] by constructing an exact lattice duality mapping of the *full* Hilbert space of the underlying spins onto a dual space of spinons and visons *without* imposing any local \mathbb{Z}_2 conservation laws that would freeze the motion of these particles. Namely, we will construct nonlocal spinon and vison creation/annihilation operators in a completely explicit form in terms of underlying spin-1/2 operators. One of the key properties of our construction is that the dual Hilbert space completely “disentangles” the vison and emergent fermion degrees of freedom, in the sense that the dual states can be organized as tensor products of vison and emergent fermion configurations. We will use this construction to compute the Berry phases associated with transporting the vison around plaquettes in closed loops in the background of topological superconducting state of the spinons with a nonzero Chern number. Throughout this paper we will refer to the vison π -flux excitations sometimes as “ e particles” and the fermionic spinons as the “ ε particles.” A recent work [12] computed these phases when the fermions were in Bogoliubov–de Gennes (BdG) states with zero Chern number, relying on the property that these could be realized as ground states of commuting projector Hamiltonians. But it is known that chiral states cannot be realized in this fashion [19], and, therefore, our current approach overcomes these limitations.

The rest of the paper is organized as follows: Sec. II contains the theoretical foundation of this paper, which is an exact

*sodemann@itp.uni-leipzig.de

Published by the American Physical Society under the terms of the [Creative Commons Attribution 4.0 International license](https://creativecommons.org/licenses/by/4.0/). Further distribution of this work must maintain attribution to the author(s) and the published article’s title, journal citation, and DOI. Open access publication funded by the Max Planck Society.

duality mapping of a 2D spin system and a Hilbert space of mutual semions. In Sec. II A, we introduce the duality mapping where the dual space consists of e (boson) and m (boson) particles; in Sec. II B, we introduce the mapping with the dual space containing visons (e boson) and spinons (ε fermion). As an application of this new theoretical tool, we computed the vison Berry phases for the celebrated Kitaev model. The model (and its dual form) were briefly reviewed in Sec. III. Our main results are presented in Sec. IV: Sec. IV A shows the results for the Kitaev model with a finite spinon Haldane mass term, and the results for a model with a higher spinon Chern number ($C = -2$) are presented in Sec. IV B. We summarize and discuss our findings in Sec. V.

II. DUALITY MAPPING

A. Boson-boson mapping

In this section, we will illustrate the idea of the boson-boson mapping. For simplicity, here we will focus on the case of an *infinite* system, the mappings on an open and a periodic system are provided in the Supplemental Material [20].

As has been shown explicitly in the TC model [9] for a 2D spin system with spins residing on the links of a square lattice (its Hilbert space will be denoted as $\mathcal{H}_{\text{spin}}$), one can define the so-called star and plaquette operators associated with each vertex and plaquette respectively,

$$A_v = \prod_{l \in \text{star}(v)} X_l, \quad B_p = \prod_{l \in \text{boundary}(p)} Z_l. \quad (1)$$

All the A_v 's and B_p 's commute with each other, moreover, the eigenstates of them form a basis of the spin Hilbert space $\mathcal{H}_{\text{spin}}$. One can define a dual spin system $\mathcal{H}_{e\text{-spin}} \times \mathcal{H}_{m\text{-spin}}$ containing two types of *spins*, denoted as e and m spins. Here the e and m spins sit on the vertices and plaquettes of the square lattice, respectively, whose spin- Z configurations are related to the occupation of the e and m particles (see below). The local spin- X and $-Z$ Pauli matrices of the dual e (m) spins are denoted as X_v^e (X_p^m) and Z_v^e (Z_p^m), which satisfy the following commutation relations:

$$[X_v^e, Z_{v'}^e] = 0 \quad (v \neq v'), \quad \{X_v^e, Z_v^e\} = 0, \quad (2a)$$

$$[Z_p^m, X_{p'}^m] = 0 \quad (p \neq p'), \quad \{Z_p^m, X_p^m\} = 0, \quad (2b)$$

$$[X_v^e, X_p^m] = [Z_v^e, Z_p^m] = [X_v^e, Z_p^m] = [Z_v^e, X_p^m] = 0. \quad (2c)$$

Within the duality mapping, we will map the eigenbases of A_v and B_p from $\mathcal{H}_{\text{spin}}$ to the local spin- Z eigenbasis of e and m spins such that the star and plaquette operators are mapped to the spin- Z Pauli matrices of e and m spins, respectively,

$$A_v \leftrightarrow Z_v^e, \quad B_p \leftrightarrow Z_p^m. \quad (3)$$

To make the dual operators of X_v^e , Z_v^e , X_p^m , and Z_p^m should also satisfy the algebraic relations in Eq. (2), we found that the following choice of dual operators do the job:

$$\prod_{l \in R(v)} Z_l \leftrightarrow X_v^e, \quad \prod_{l \in L(p)} X_l \leftrightarrow X_p^m. \quad (4)$$

Here $R(v)$ stands for the horizontal links to the right of vertex v , $L(p)$ stands for the vertical links to the left of plaquette p [see Fig. 1(a) for a schematic of the nonlocal operators above].

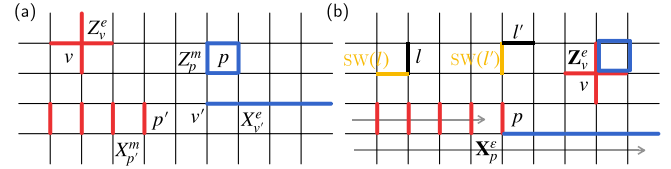


FIG. 1. Schematic of the infinite system for both boson-boson and boson-fermion mappings. (a) Operators for the boson-boson mapping (infinite lattice). Spin- X ($-Z$) operators at each link are represented by red (blue) colored bonds. (b) Operators for the boson-fermion mapping (infinite lattice). The gray arrow indicates the sequence of plaquettes in the Jordan-Wigner transformation, which increases from lower to upper rows.

It can be shown that the local spin- X and $-Z$ operators in $\mathcal{H}_{\text{spin}}$ can be mapped to

(i) Vertical l ,

$$X_l \leftrightarrow X_{p_1}^m X_{p_2}^m, \quad Z_l \leftrightarrow X_{v_1}^e X_{v_2}^e \prod_{p \in R(l)} Z_p^m. \quad (5)$$

(ii) Horizontal l ,

$$X_l \leftrightarrow X_{p_1}^m X_{p_2}^m \prod_{v \in L(l)} Z_v^e, \quad Z_l \leftrightarrow X_{v_1}^e X_{v_2}^e. \quad (6)$$

Here for any vertical (horizontal) link l , the two vertices connected by it are denoted as v_1 and v_2 , the plaquettes to its left (top) and right (bottom) are called p_1 and p_2 . $L(l)$ stands for vertices to the left of a horizontal l (including v_1). Note that spin- X_l and $-Z_l$ operators form a complete algebraic basis out of which any other spin operators can be written in terms of their summation, products and multiplication with complex numbers. In this way, we have established the duality mapping between $\mathcal{H}_{\text{spin}}$ and $\mathcal{H}_{e\text{-spin}} \times \mathcal{H}_{m\text{-spin}}$.

Since spin-1/2 degrees of freedom can be equivalently viewed as hard-core (e and m) bosons, it is straightforward to establish the mapping $\mathcal{H}_{e\text{-spin}} \times \mathcal{H}_{m\text{-spin}} \leftrightarrow \mathcal{H}_e \times \mathcal{H}_m$, the e and m spins' Pauli matrices can be written as bosonic operators,

$$Z_v^e \leftrightarrow (-1)^{b_v^\dagger b_v}, \quad X_v^e \leftrightarrow (b_v + b_v^\dagger), \quad (7a)$$

$$Z_p^m \leftrightarrow (-1)^{d_p^\dagger d_p}, \quad X_p^m \leftrightarrow (d_p + d_p^\dagger). \quad (7b)$$

Here b_v (d_p) is the annihilation operator of an e (m) boson at vertex v (plaquette p).

Finally, we obtain the duality mapping between $\mathcal{H}_{\text{spin}}$ and $\mathcal{H}_e \times \mathcal{H}_m$ where the star and plaquettes operators of the original spin space are mapped to the parity operators of e and m bosons,

$$A_v \leftrightarrow (-1)^{b_v^\dagger b_v}, \quad B_p \leftrightarrow (-1)^{d_p^\dagger d_p}. \quad (8)$$

The local spin operators are mapped into

(i) Vertical l ,

$$X_l \leftrightarrow (d_{p_1} + d_{p_1}^\dagger)(d_{p_2} + d_{p_2}^\dagger), \quad (9)$$

$$Z_l \leftrightarrow (b_{v_1} + b_{v_1}^\dagger)(b_{v_2} + b_{v_2}^\dagger) \prod_{p \in R(l)} (-1)^{d_p^\dagger d_p}. \quad (10)$$

(ii) Horizontal l ,

$$X_l \leftrightarrow \prod_{v \in L(l)} (-1)^{b_v^\dagger b_v} (d_{p_1} + d_{p_1}^\dagger)(d_{p_2} + d_{p_2}^\dagger), \quad (11)$$

$$Z_l \leftrightarrow (b_{v_1} + b_{v_1}^\dagger)(b_{v_2} + b_{v_2}^\dagger). \quad (12)$$

Within this duality mapping, local Z_l (X_l) operators have the effect of pair fluctuating and hopping the e (m) particles on nearest-neighbor vertices v_1 and v_2 (plaquettes p_1 and p_2) as one would naturally expect since they anticommute with the e (m) particles' parity operator at those two vertices (plaquettes). More interestingly, there is also a product of m (e) particles' parity operators when the e (m) particle is hopping along the y direction [21], such nonlocal statistical interaction terms make the e and m particles mutual semi-ions.

B. Boson-fermion mapping

1. Infinite lattice

It turns out that it is also possible to map the $\mathcal{H}_{\text{spin}}$ to a space of bosons (e particles) and fermions (ε particles) $\mathcal{H}_e \times \mathcal{H}_\varepsilon$. For a pedagogical reason, we will start with the case with an infinite lattice and introduce the mapping on a periodic system in the next section. The mapping for an open lattice can be found in the Supplemental Material [20].

Each ε particle in the boson-fermion mapping can be viewed as a composite of e and m particles of the boson-boson mapping, and the e and ε particles are mutual semions [9]. The same as the boson-boson mapping introduced in the previous section, the mapping between $\mathcal{H}_{\text{spin}}$ and $\mathcal{H}_e \times \mathcal{H}_\varepsilon$ can be made more obvious if one first introduces an intermediate dual spin space $\mathcal{H}_{e\text{-spin}} \times \mathcal{H}_{\varepsilon\text{-spin}}$, where the e (ε) spins are located at the vertices (plaquettes) of a square lattice. Recall that the eigenstates of A_v and B_p are also eigenstates of all the $A_v B_{p(v)}$'s and B_p 's. Here $p(v)$ stands for the plaquettes to the northeast of vertex v . One can map this eigenbasis to the local spin- Z eigenbases of e and ε spins of the intermediate dual space such that

$$A_v B_{p(v)} \leftrightarrow \mathbf{Z}_v^e, \quad B_p \leftrightarrow \mathbf{Z}_p^\varepsilon. \quad (13)$$

Note that here we used bold symbols to denote the Pauli matrices of the e and ε spins, which satisfy the following algebraic relations:

$$[\mathbf{X}_v^e, \mathbf{Z}_{v'}^e] = 0 \quad (v \neq v'), \quad \{\mathbf{X}_v^e, \mathbf{Z}_v^e\} = 0, \quad (14a)$$

$$[\mathbf{Z}_p^\varepsilon, \mathbf{X}_{p'}^\varepsilon] = 0 \quad (p \neq p'), \quad \{\mathbf{Z}_p^\varepsilon, \mathbf{X}_p^\varepsilon\} = 0, \quad (14b)$$

$$[\mathbf{Z}_v^e, \mathbf{Z}_p^\varepsilon] = [\mathbf{X}_v^e, \mathbf{X}_p^\varepsilon] = [\mathbf{X}_v^e, \mathbf{Z}_p^\varepsilon] = [\mathbf{Z}_v^e, \mathbf{X}_p^\varepsilon] = 0. \quad (14c)$$

In $\mathcal{H}_{\text{spin}}$, the dual operators of \mathbf{X}_v^e and \mathbf{X}_p^ε will respect these relations if one chooses

$$\prod_{l \in R(v)} Z_l \leftrightarrow \mathbf{X}_v^e, \quad (15)$$

$$\prod_{l \in R(v(p))} Z_l \prod_{l' \in L(p)} X_{l'} \leftrightarrow \mathbf{X}_p^\varepsilon. \quad (16)$$

Here $v(p)$ stands for the vertex to the southwest of plaquette p . A schematic of these nonlocal spin operators are shown

in Fig. 1(b). In this way, we have completed the mapping between $\mathcal{H}_{\text{spin}}$ and $\mathcal{H}_{e\text{-spin}} \times \mathcal{H}_{\varepsilon\text{-spin}}$.

The mapping from $\mathcal{H}_{e\text{-spin}} \times \mathcal{H}_{\varepsilon\text{-spin}}$ to $\mathcal{H}_e \times \mathcal{H}_\varepsilon$ is more straightforward, the e particles are just the hard-core boson corresponding to the e spins, and the $\mathcal{H}_{\varepsilon\text{-spin}}$ is mapped to \mathcal{H}_ε through a Jordan-Wigner transformation,

$$\mathbf{Z}_v^e \leftrightarrow (-1)^{b_v^\dagger b_v}, \quad \mathbf{X}_v^e \leftrightarrow (b_v + b_v^\dagger), \quad (17)$$

$$\mathbf{Z}_p^\varepsilon \leftrightarrow -i\gamma_p \gamma_p', \quad \mathbf{X}_p^\varepsilon \leftrightarrow \left(\prod_{q < p} -i\gamma_q \gamma_q' \right) \gamma_p'. \quad (18)$$

Here b_v (b_v^\dagger) is the annihilation (creation) operator for the e particle at vertex v . We have also introduced two Majorana fermion modes (γ_p and γ_p') to represent the complex ε fermion mode (whose annihilation/creation operator is c_p/c_p^\dagger) at each plaquette p with

$$\gamma_p = c_p + c_p^\dagger, \quad \gamma_p' = \frac{1}{i}(c_p - c_p^\dagger). \quad (19)$$

Note that the fermion parity at each plaquette p is $(-1)^{c_p^\dagger c_p} = -i\gamma_p \gamma_p'$. The sequence of plaquettes in the Jordan-Wigner transformation is indicated by the gray arrow in Fig. 1(b). In this way, we have established the mapping between $\mathcal{H}_{\text{spin}}$ and $\mathcal{H}_e \times \mathcal{H}_\varepsilon$, it can be shown that the following local spin operators are mapped to:

(i) l is a vertical link,

$$X_{l\text{SW}(l)} \leftrightarrow \mathbf{X}_{p_1}^e \mathbf{X}_{p_2}^e \leftrightarrow i\gamma_{p_1} \gamma_{p_2}', \quad (20)$$

$$Z_l \leftrightarrow \mathbf{X}_{v_1}^e \mathbf{X}_{v_2}^e \prod_{p \in R(l)} \mathbf{Z}_p^\varepsilon \\ \leftrightarrow (b_{v_1} + b_{v_1}^\dagger)(b_{v_2} + b_{v_2}^\dagger) \prod_{p \in R(l)} (-i\gamma_p \gamma_p'). \quad (21)$$

(ii) l is a horizontal link,

$$X_{l\text{SW}(l)} \leftrightarrow (-1) \prod_{v \in L(l)} \mathbf{Z}_v^e \left(\prod_{p_2 \leq p \leq p_1} \mathbf{Z}_p^\varepsilon \right) \mathbf{X}_{p_1}^e \mathbf{X}_{p_2}^e \\ \leftrightarrow \prod_{v \in L(l)} (-1)^{b_v^\dagger b_v} i\gamma_{p_1} \gamma_{p_2}'. \quad (22)$$

$$Z_l \leftrightarrow \mathbf{X}_{v_1}^e \mathbf{X}_{v_2}^e \leftrightarrow (b_{v_1} + b_{v_1}^\dagger)(b_{v_2} + b_{v_2}^\dagger). \quad (23)$$

Here $\text{SW}(l)$ is the link to the southwest of link l , which also connects to it [see Fig. 1(b) for a schematic]. It is clear that the local Z_l ($X_{l\text{SW}(l)}$) operator is able to pair create, annihilate, and hop the e (ε) particles in the nearest neighbors. The nonlocal products of the e -particle (ε -particle) parities in the dual operator of $X_{l\text{SW}(l)}$ (Z_l) indicate the statistical interaction between e and ε particles, which view each other as π fluxes, i.e., they are mutual semi-ions.

2. Periodic lattice

The idea of the duality mapping on a periodic lattice (torus) is basically the same as the infinite lattice case. However, there

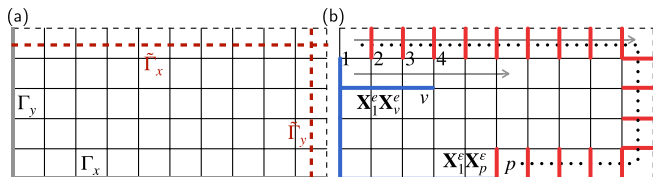


FIG. 2. Schematic of operators in the boson-fermion mapping for a periodic lattice. (a) Noncontractible loops used in the definition of the Wilson loop and t'Hooft operators. $\Gamma_{x/y}$ is highlighted in gray color, and $\tilde{\Gamma}_{x/y}$ is highlighted in red color. (b) The dual of $\mathbf{X}_1^e \mathbf{X}_v^e$ and $\mathbf{X}_1^e \mathbf{X}_p^e$ operators. The sequence of vertices and the associated plaquettes (to the northeast of each vertex) starts with the one on the top left, ascends towards the right direction within each row and increases from the top to bottom rows as indicated by the gray arrow. The $\Gamma_{1,v}$ path starts from vertex 1, goes down first then goes to the right direction until reaching vertex v , see the path paved by blue colored bonds. The dual path $\tilde{\Gamma}_{1,p}$ starts from plaquette 1, goes to the right end first, then goes down, and finally goes left until plaquette p . An example is indicated by the black dotted line in the figure.

are now two global constraints in the original spin space,

$$\prod_v A_v B_{p(v)} = 1, \quad \prod_p B_p = 1. \quad (24)$$

Therefore, only an even number of $A_v B_{p(v)}$ and B_p can take -1 , i.e., there are only $2^{2\mathcal{N}-2}$ different configurations of $A_v B_{p(v)}$ and B_p , where \mathcal{N} is the number of unit cells in the system. To fully characterize the spin Hilbert space (with dimension $2^{2\mathcal{N}}$), one needs to introduce two additional Wilson loop degrees of freedom. The Wilson loop operators commute with all the $A_v B_{p(v)}$ and B_p operators, one possible choice is as follows:

$$W_1 = - \prod_{l \in \tilde{\Gamma}_x} X_l \prod_{l' \in \Gamma_x} Z_{l'}, \quad W_2 = - \prod_{l \in \tilde{\Gamma}_y} X_l \prod_{l' \in \Gamma_y} Z_{l'}. \quad (25)$$

Here $l \in \tilde{\Gamma}_{x/y}$ denotes the link l crossing the dual-lattice path $\tilde{\Gamma}_{x/y}$. Paths $\Gamma_{x,y}$ and $\tilde{\Gamma}_{x,y}$ are shown in Fig. 2(a). $W_{1/2}$ takes the value of ± 1 and can be interpreted as a closed transport of ε particles across a x/y -oriented noncontractible loop of the torus (see below). One can also define two t'Hooft operators T_1 and T_2 which commutes with all the $A_v B_{p(v)}$ and B_p but, respectively, anticommutes with W_1 and W_2 , which read

$$T_1 = \prod_{l \in \Gamma_y} Z_l, \quad T_2 = \prod_{l \in \Gamma_x} Z_l. \quad (26)$$

As will become clear later, $T_{1/2}$ plays the role of transporting an e particle across the y/x -oriented noncontractible loop of the torus.

The intermediate dual (spin) space for a periodic system reads $\mathcal{H}_{e\text{-spin}}^{\text{even}\downarrow} \times \mathcal{H}_{\varepsilon\text{-spin}}^{\text{even}\downarrow} \times \mathcal{H}_W$. Here $\mathcal{H}_{e\text{-spin}}^{\text{even}\downarrow}$ stands for the even- \downarrow subspace of the e spins (same for the $\mathcal{H}_{\varepsilon\text{-spin}}^{\text{even}\downarrow}$) due to the constraint Eq. (24). \mathcal{H}_W is a four-dimensional Hilbert space containing two (auxiliary) spins, which we call Wilson loop spins (WLS) as they correspond to the two Wilson loop degrees of freedom in the original spin system. When establishing the mapping between $\mathcal{H}_{\text{spin}}$ and $\mathcal{H}_{e\text{-spin}}^{\text{even}\downarrow} \times \mathcal{H}_{\varepsilon\text{-spin}}^{\text{even}\downarrow} \times \mathcal{H}_W$, the eigenbases of all the $A_v B_{p(v)}$, B_p , and $W_{1,2}$ will be

mapped to the spin Z eigenbasis of e spins, ε spins, and WLS, which gives

$$A_v B_{p(v)} \leftrightarrow Z_v^e, \quad B_p \leftrightarrow Z_p^\varepsilon, \quad W_{1,2} \leftrightarrow Z_{1,2}^W. \quad (27)$$

The t'Hooft operators are mapped to the Pauli X matrices of the WLS: $T_{1,2} \leftrightarrow X_{1,2}^W$. Note that there is an implicit projection operator P in the dual spin operators, which projects states to the even- \downarrow subspace of e and ε spins. Since the physical dual spin subspace states contains only an even number of (e and ε) down spins, a single \mathbf{X}_v^e or \mathbf{X}_p^ε has no matrix element in this subspace because they only mix states with different number of down spins. On the other hand, bilinears of \mathbf{X}_v^e or \mathbf{X}_p^ε have nonzero matrix elements in the physical subspace. For convenience, we take vertex/plaquette 1 as a ‘‘reference’’ vertex/plaquette [see Fig. 2(b)] and looked for the dual operators of $\mathbf{X}_1^e \mathbf{X}_v^e$ and $\mathbf{X}_1^e \mathbf{X}_p^\varepsilon$ such that the algebraic relations in Eq. (14) can be satisfied. One possible choice is the following mapping:

$$\prod_{l \in \Gamma_{1,v}} Z_l \leftrightarrow \mathbf{X}_1^e \mathbf{X}_v^e, \quad (28)$$

$$\prod_{l \in \Gamma_{1,v}} Z_l \prod_{l' \in \tilde{\Gamma}_{1,p}} X_{l'} \leftrightarrow \mathbf{X}_1^e \mathbf{X}_p^\varepsilon \quad (29)$$

Here $\Gamma_{1,v}$ ($\tilde{\Gamma}_{1,p}$) is a direct (dual) lattice path connecting the vertices 1 and v (plaquettes 1 and p), see Fig. 2(b) for a schematic of them. To simplify the notation, we are simply using the sequence numbers of vertices and plaquettes to denote them in the subindices of the operators [see their order in Fig. 2(b)].

The mapping from e spins (ε spins) to the e bosons (ε fermions) is very similar to the infinite lattice case shown in Eqs. (17) and (18), however, due to the constraints in Eq. (24), the (physical) e - and ε -particle states contain only an even number of particles. The dual boson-fermion (and WLS) space reads $\mathcal{H}_e^{\text{even}} \times \mathcal{H}_\varepsilon^{\text{even}} \times \mathcal{H}_W$. Note that the sequence of plaquettes in the Jordan-Wigner transformation between ε spins and ε fermions has also changed now [which is shown in Fig. 2(b)]. In this way, one obtains the duality mapping between $\mathcal{H}_{\text{spin}}$ and $\mathcal{H}_e^{\text{even}} \times \mathcal{H}_\varepsilon^{\text{even}} \times \mathcal{H}_W$, local X_l and $X_l Z_{\text{SW}(l)}$ operators are mapped to

(I) l is a vertical link,

(i) $l \notin \Gamma_y$, and l does not cross $\tilde{\Gamma}_x$,

$$Z_l \leftrightarrow (b_{v_1} + b_{v_1}^\dagger)(b_{v_2} + b_{v_2}^\dagger) \left(\prod_{l' \in \tilde{\Gamma}_{1,p}} -i\gamma_p \gamma_p' \right), \quad (30a)$$

$$X_l Z_{\text{SW}(l)} \leftrightarrow i\gamma_p \gamma_p'. \quad (30b)$$

(ii) $l \in \Gamma_y$, and l does not cross $\tilde{\Gamma}_x$,

$$Z_l \leftrightarrow (b_{v_1} + b_{v_1}^\dagger)(b_{v_2} + b_{v_2}^\dagger), \quad (31a)$$

$$X_l Z_{\text{SW}(l)} \leftrightarrow \left[\prod_{l' \in \Gamma_{1,v}} (-1)^{b_{v'}^\dagger b_{v'}} \right] i\gamma_{p_1} \gamma_{p_2}' Z_1^W. \quad (31b)$$

(iii) $l \notin \Gamma_y$, and l crosses $\tilde{\Gamma}_x$,

$$Z_l \leftrightarrow (b_{v_1} + b_{v_1}^\dagger)(b_{v_2} + b_{v_2}^\dagger) \left(\prod_{l \times \tilde{\Gamma}_{1,p}} -i\gamma_p \gamma'_p \right) X_1^W, \quad (32a)$$

$$X_l Z_{SW(l)} \leftrightarrow i\gamma_{p_1} \gamma'_{p_2}. \quad (32b)$$

(iv) $l \in \Gamma_y$, and l crosses $\tilde{\Gamma}_x$,

$$Z_l \leftrightarrow (b_{v_1} + b_{v_1}^\dagger)(b_{v_2} + b_{v_2}^\dagger) X_1^W, \quad (33a)$$

$$X_l Z_{SW(l)} \leftrightarrow i\gamma_p \gamma'_p Z_1^W. \quad (33b)$$

(II) l is a horizontal link,

(i) $l \notin \Gamma_x$, and l does not cross $\tilde{\Gamma}_y$,

$$Z_l \leftrightarrow (b_{v_1} + b_{v_1}^\dagger)(b_{v_2} + b_{v_2}^\dagger), \quad (34a)$$

$$X_l Z_{SW(l)} \leftrightarrow \left[\prod_{l \in \Gamma_{1,v}} (-1)^{b_v^\dagger b_v} \right] i\gamma_{p_1} \gamma'_{p_2}. \quad (34b)$$

(ii) $l \in \Gamma_x$, and l does not cross $\tilde{\Gamma}_y$,

$$Z_l \leftrightarrow (b_{v_1} + b_{v_1}^\dagger)(b_{v_2} + b_{v_2}^\dagger), \quad (35a)$$

$$X_l Z_{SW(l)} \leftrightarrow \left[\prod_{l \in \Gamma_{1,v}} (-1)^{b_v^\dagger b_v} \right] i\gamma_{p_1} \gamma'_{p_2} Z_2^W. \quad (35b)$$

(iii) $l \notin \Gamma_x$, and l crosses $\tilde{\Gamma}_y$,

$$Z_l \leftrightarrow (b_{v_1} + b_{v_1}^\dagger)(b_{v_2} + b_{v_2}^\dagger) \left(\prod_{l \times \tilde{\Gamma}_{1,p}} -i\gamma_p \gamma'_p \right) X_2^W, \quad (36a)$$

$$X_l Z_{SW(l)} \leftrightarrow i\gamma_{p_1} \gamma'_{p_2}. \quad (36b)$$

(iv) $l \in \Gamma_x$, and l crosses $\tilde{\Gamma}_y$,

$$Z_l \leftrightarrow (b_{v_1} + b_{v_1}^\dagger)(b_{v_2} + b_{v_2}^\dagger) X_2^W, \quad (37a)$$

$$X_l \leftrightarrow i\gamma_{p_1} \gamma'_{p_2} Z_2^W. \quad (37b)$$

Here for a horizontal (vertical) link l , v_1 and v_2 are the two vertices connected by it, p_1 and p_2 are the plaquettes to its top (left) and bottom (right). Again, the nonlocal boson and fermion parities in the dual operators reflect the semionic statistical interaction between e and ε particles. Moreover, when an e (ε) particle is moving across the x/y direction boundary, there will be an associated $X_{2/1}^W$ ($Z_{1/2}^W$) operator. The spin- Z configuration of WLS determines the boundary condition of ε particles.

III. MODEL HAMILTONIAN

In this paper, we consider Hamiltonians of the form $H = H_0 + H_1$. H_0 commutes with $A_v B_{p(v)}$ for $\forall v$, according to the boson-fermion mapping introduced in Sec. II B, its dual operator has dynamical (ε) fermions and static π fluxes (e particles). Many exactly solvable models can be constructed from these type of Hamiltonians by making the

fermions free, e.g., the Kitaev honeycomb model [10–13]. H_1 will be a term that allows the motion of e particles, whereas preserving their total number. We choose H_0 to be given by

$$\begin{aligned} H_0 = & \sum_{l \in h\text{-link}} -J_x X_l Z_{SW(l)} + J_y Y_l Y_{SE(l)} - J_z X_{NE(l)} Z_l \\ & + \kappa [Z_l Z_{SW(l)} Y_{SE(l)} + X_l X_{NE(l)} Y_{SE(l)} - Y_l Z_{SE(l)} X_{NE(l)}] \\ & + \sum_{l \in v\text{-link}} \kappa [Y_l Z_{SW(l)} X_{NE(l)} - Z_l Z_{SW(l)} Y_{NW(l)} \\ & - X_l X_{NE(l)} Y_{NW(l)}]. \end{aligned} \quad (38)$$

Here the h/v link stands for horizontal/vertical links. This Hamiltonian is equivalent to the Kitaev honeycomb Hamiltonian (with a Haldane mass term κ) [13] by placing the sites of the original honeycomb lattice onto the links of a square lattice (see Supplemental Material Sec. S III [20] for a schematic of the lattice) and a unitary transformation U which transforms

$$X_j \leftrightarrow Z_j, \quad Y_j \rightarrow -Y_j, \quad \forall j \in A \text{ sublattice}. \quad (39)$$

Under the duality transformation introduced in Sec. II B, the dual Hamiltonian reads (for an infinite system)

$$\begin{aligned} \tilde{H}_0 = & - \sum_p (J_x e^{i\pi \beta_{\mathbb{L}(p,p+\hat{y})}} i\gamma_{p+\hat{y}} \gamma'_p \\ & + J_y e^{i\pi \beta_{\mathbb{L}(p,p+\hat{x})}} i\gamma_{p+\hat{x}} \gamma'_{p+\hat{x}} + J_z i\gamma_p \gamma'_{p+\hat{x}}) \\ & - \kappa \sum_p [e^{i\pi \beta_{\mathbb{L}(p,p+\hat{y})}} i\gamma_{p+\hat{y}} \gamma_{p-\hat{x}} \\ & + e^{i\pi \beta_{v(p)} b_{v(p)}} i\gamma_{p-\hat{x}} \gamma_p + e^{i\pi \beta_{\mathbb{L}(p,p+\hat{y})}} i\gamma_p \gamma_{p+\hat{y}} \\ & + e^{i\pi \beta_{\mathbb{L}(p-\hat{x},p-\hat{x}+\hat{y})}} i\gamma'_{p+\hat{y}} \gamma'_p \\ & + i\gamma'_{p+\hat{x}} \gamma'_p + e^{i\pi \beta_{\mathbb{L}(p,p-\hat{y})}} i\gamma'_{p-\hat{y}} \gamma'_{p+\hat{x}}]. \end{aligned} \quad (40)$$

Here $\mathbb{L}(p, p')$ stands for the link sandwiched by plaquettes p and p' , $\beta_l = \sum_{v \in L(l)} b_v^\dagger b_v$ for a horizontal link l [here $L(l)$ stands for the vertices to the left of link l]. It is clear that \tilde{H}_0 has a BdG form for the ε fermions in a background of static π fluxes (e particles) and can be solved exactly within any given real-space configuration of e particles.

As for H_1 , we choose it to be as follows:

$$H_1 = g \sum_l Z_l \frac{1 - A_{v_1(l)} B_{p[v_1(l)]} A_{v_2(l)} B_{p[v_2(l)]}}{2}, \quad (41)$$

with $v_1(l)$ and $v_2(l)$ being the two vertices adjacent to link l . Its dual operator \tilde{H}_1 , according to Eqs. (17) and (23) reads (for the infinite lattice case),

$$\tilde{H}_1 = g \sum_v b_v^\dagger b_{v+\hat{y}} \prod_{p \in R[\mathbb{L}(v, v+\hat{y})]} (-i\gamma_p \gamma'_p) + b_v^\dagger b_{v+\hat{x}} + \text{H.c.} \quad (42)$$

$\sim b_{v_1}^\dagger b_{v_2} + b_{v_2}^\dagger b_{v_1}$, Here $\mathbb{L}(v, v')$ stands for the link connecting vertices v and v' , $R(l)$ stands for the plaquettes to the link l . Note that the above Hamiltonian is a sum of operators that act on spins contained within some local region of the link l , and, therefore, it is a strictly local perturbation (even though

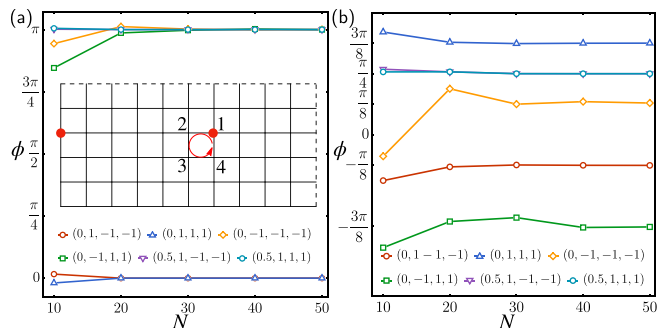


FIG. 3. Berry phase for e particles. (a) Berry phase for a single-plaquette movement of an e particle. $\phi \rightarrow 0$ or π in the thermodynamic limit. The inset indicates the setup of numerical calculations: two e particles are highlighted by the red dots with one of them hops circularly between the four sites. The legends indicate values of parameters (t, J_y, z_1, z_2) in the model. (b) Berry phase for the exchange of two e particles. ϕ converges to predicted values in Ref. [13] as $N \rightarrow \infty$.

it contains products of several spin operators). So \tilde{H}_1 contains nearest-neighbor e -particle hopping terms. Note that it is also dressed by ε particles' parities due to the statistical interaction between e and ε particles. To perform calculations, in this paper, H_1 will be treated as a perturbation to H_0 .

IV. BERRY PHASES OF VISONS

A. Kitaev model with a Haldane mass term

We will use the previously described mapping to compute the Berry phase for transporting the π flux in a closed loop around a single plaquette. This phase can be viewed as a universal characterization of the topologically ordered state enriched by lattice translational symmetry [22–28].

In order to compute the Berry phase, we place two e particles far apart on a torus and will allow only one of them to move within the four vertices surrounding a plaquette [see the inset to Fig. 3(a)]. This is accomplished by only adding the flux-hopping operator from Eq. (41) to be nonzero at the links connecting these four vertices. For a fixed WLS configuration $|z_1, z_2\rangle$, when the mobile e particle is located at site $j \in \{1-4\}$, the corresponding *physical* (even number of ε particles) ground state of \tilde{H}_0 reads

$$|\Phi_j\rangle = b_0^\dagger b_j^\dagger |0\rangle \otimes |\Psi_j^\varepsilon\rangle \otimes |z_1, z_2\rangle. \quad (43)$$

Here $|\Psi_j^\varepsilon\rangle$ is the even-parity ground state of a BdG Hamiltonian with two π fluxes at 0 and j , and the $z_{1,2} = \pm 1$ are the eigenvalues of the Wilson loop operators that label the global periodic/antiperiodic boundary conditions of the fermions along the x and y directions (see Supplemental Material Sec. S III [20]). $|\Psi_j^\varepsilon\rangle$ can be solved exactly and has a BCS form (see Supplemental Material [20]). The Berry phase for this close-loop movement of an e particle is as follows: $e^{i\phi} \approx \prod_{j=1}^4 \langle \Phi_{j+1} | Z_{j+1,j} | \Phi_j \rangle$. Note that the index j runs

cyclically from 1 to 4, i.e., $|\Phi_5\rangle \equiv |\Phi_1\rangle$. In the dual space, the Berry phase reads

$$e^{i\phi} = \langle \Psi_1^\varepsilon | \left(\prod_{p \in L(4,1)} -i\gamma_p \gamma'_p \right) | \Psi_4^\varepsilon \rangle \langle \Psi_4^\varepsilon | \Psi_3^\varepsilon \rangle \times \langle \Psi_3^\varepsilon | \left(\prod_{p \in L(3,2)} -i\gamma_p \gamma'_p \right) | \Psi_2^\varepsilon \rangle \langle \Psi_2^\varepsilon | \Psi_1^\varepsilon \rangle. \quad (44)$$

Here $L(4, 1)$ denotes the string of plaquettes to the left of link $(4,1)$ that runs until the left edge of the torus.

In our paper, we take the following parameters: $J_x = J_z = 1$, $\kappa = 0.1$. The torus has $N \times N$ plaquettes with N even. We consider two values $J_y = \pm 1$ which corresponds to fermionic BdG states with Chern numbers $C = \pm 1$. There are four high-symmetry points (HSPs) in k space which are unpaired in a BdG Hamiltonian [12,29,30]: $(0, 0)$, $(\pi, 0)$, $(0, \pi)$, and (π, π) . For $J_y = 1$, the fermion band energy $\epsilon(0, 0) < 0$ and is positive at other three HSPs. In this case, we have found that the single-plaquette Berry phase $\phi \rightarrow 0$ with increasing N for any BC. On the other hand, for $J_y = -1$, $\epsilon(\mathbf{k}) < 0$ at $(0,0)$, $(\pi, 0)$, and $(0, \pi)$ and is positive at (π, π) . For this case we have found that for any BC, $\phi \rightarrow \pi$ as N increases. The results are presented in Fig. 3(a) and this is one of the main findings of our paper.

The motion of the vison in the ferromagnetic (FM) and antiferromagnetic (AFM) Kitaev models induced by physically realistic perturbations, such as the Zeemann field, has also been studied in Refs. [31,32]. Whereas an earlier version of Ref. [31] had concluded that the phase of vison in the FM model was π around a unit cell, the updated understanding provided in Refs. [31,32] is currently in mutual agreement with the conclusion that the vison acquires zero phase in the FM model and π phase in the AFM model around a unit cell, which is also in agreement with the current paper.

We also studied the braiding phases for two anyons. To avoid geometric phases depending on the details of the braiding path, we follow the Levin-Wen protocol [13,33,34]. Figure 3(b) presents results of the braiding phases. For $J_y = 1$ with increasing system size, the braiding phase $\phi \rightarrow -\pi/8$ for antiperiodic BC (APBC) and $\phi \rightarrow 3\pi/8$ for periodic BC (PBC). Whereas for $J_y = -1$, the $\phi \rightarrow \pi/8$ for APBC and $\phi \rightarrow -3\pi/8$ for PBC. Our results for ϕ match exactly the prediction of $R_1^{\sigma,\sigma} \propto \exp(-iC\pi/8)$ and $R_\varepsilon^{\sigma,\sigma} \propto \exp(iC3\pi/8)$ in Ref. [13] (here σ stands for the π -flux particle). The difference between PBC and APBC originates from the fermion ground-state parity of \tilde{H}_0 . The state with $J_y = 1$ is a $p + ip$ topological superconductor, and the ground state would have an odd number of fermions under PBC [35], which is unphysical in our case. Since, only even-parity states are physical, the lowest-energy physical eigenstate of \tilde{H}_0 in this case is actually the first excited state of the BdG Hamiltonian with a single Bogoliubov quasiparticle. Thus, for PBCs the π fluxes are in the fusion sector $\sigma \times \sigma = \varepsilon$, explaining the difference in braidings that we observe in Fig. 3. As for APBC, the ground state of the BdG Hamiltonian contains an even number of fermions, therefore, the π fluxes are in the fusion sector $\sigma \times \sigma = 1$.

B. Higher Chern numbers and conjecture for the arbitrary case

One can also explore cases with higher Chern numbers by correspondingly modifying H_0 . This illustrates the power of this construction allowing to write an exactly solvable model for any free fermion Hamiltonian of interest. We accomplished this explicitly by introducing some four-spin interaction terms to H_0 in Eq. (38),

$$\begin{aligned} & \frac{t}{2} \left[\sum_{l \in h \text{ link}} (Y_l Z_{SW(l)} Z_{NE(l)} Y_{N(l)} + Y_l Y_{W(l)} X_{SW(l)} X_{NE(l)}) \right. \\ & + \sum_{l \in v \text{ link}} (Y_l Y_{S(l)} X_{SW(l)} X_{NE(l)} + Y_l Y_{E(l)} Z_{SW(l)} Z_{NE(l)}) \\ & \left. + \sum_p B_p + \sum_v A_v \right]. \end{aligned} \quad (45)$$

The $E(l)$ [$S(l)$] stands for the link to the east (south) of l within a common plaquette. Under the duality mapping established in this paper, these new terms are mapped to third-neighbor Majorana fermion couplings of the form

$$t \sum_p (-i\gamma_p \gamma'_p - i\gamma_p \gamma'_{p+2\hat{x}} - i\gamma_p \gamma'_{p-2\hat{y}}). \quad (46)$$

Here for simplicity we have omitted the nonlocal vison parities and the WLS operators involved in some of the terms for the complete expression see Supplemental Material Sec. S III [20].

At $J_y = 1$, $t = 0.5$, \tilde{H}_0 has $C = -2$. $\epsilon_k < 0$ at all HSPs, so for both PBC and APBC, the fermion ground-state parity of \tilde{H}_0 is even. There are two types of anyons in this case [13], and we studied the sector with $a \times \bar{a} = 1$ where a and \bar{a} denote the two kinds of π -flux particles in these states. When braiding a single e particle around a plaquette, we found Berry phase $\phi = \pi$ for any BC. As for the braiding phase, we obtained $R_1^{a,\bar{a}} = e^{i\pi/4} = e^{-iC\pi/8}$, which is also consistent with Ref. [13]. More details can be found in the Supplemental Material [20].

As mentioned before, the phase ϕ acquired by a π flux upon enclosing a plaquette is an universal characteristic of the symmetry enriched topological state. BdG states of fermions with lattice translations can be classified by their Chern number, $C \in \mathbb{Z}$, and four parity indices ζ_k , which dictate whether the band is inverted ($\zeta_k = -1$) or not ($\zeta_k = 1$) in each of the four HSPs of the Brillouin zone [12,29,30,36–39]. Therefore, the value of ϕ should be a function uniquely fixed by C and ζ_k . The analytical proof of the value of ϕ in the most general case is not known to us. Reference [12] showed that when $C = 0$, $\phi = 0$ when all $\zeta_k = 1$ and $\phi = \pi$ when all $\zeta_k = -1$ (all HSPs are band inverted), in agreement with previous

arguments [23]. Reference [12] also showed that the cases with $C = 0$ and only two $\zeta_k = -1$, corresponds to states with “weak symmetry breaking” (and, thus, the π fluxes cannot be transported to adjacent vertices with local operations). We have shown here that when only one $\zeta_k = -1$ and $C = 1$ then $\phi = 0$, and when three $\zeta_k = -1$ and $C = -1$ then $\phi = \pi$. We also showed that when $C = -2$ and all four $\zeta_k = -1$, then $\phi = \pi$. This suggest the conjecture that for states with odd C and only one $\zeta_k = -1$, then $\phi = 0$ and states with three $\zeta_k = -1$ then $\phi = \pi$. For states with even C and all $\zeta_k = 1$ then $\phi = 0$ and those with all four $\zeta_k = -1$ then $\phi = \pi$ (states with even C and only two $\zeta_k = -1$ should display weak symmetry breaking of translations [12]).

V. DISCUSSIONS

We have established an *exact* mapping between a 2D spin system and a 2D boson-boson (e, m) or boson-fermion (e, ε) system where the two types of particles in the dual space are mutual semions, which generalizes the previous dual maps that relied on imposing local \mathbb{Z}_2 constraints [10]. This amounts to constructing explicit vison and spinon nonlocal creation/annihilation operators in terms of the underlying spin degrees of freedom. Based on this mapping, we found that the Berry phase for the transport of the vison (π -flux excitation) around a single plaquette was quantized to be 0 or π . We have conjectured a universal form of this phase that depends on the Chern number and the parity indices at HSPs of the BdG band structure of the spinons, generalizing previous results from nonchiral states in Refs. [12,23] to chiral and non-Abelian states. We also computed explicitly the braiding phase between two visons, which was found to be consistent with the general arguments of Ref. [13] for both $C = 1$ and $C = 2$ states of the spinons. In the models studied here, the e particles are static, and we only need to solve a free fermionic Hamiltonian of $N^2 \times N^2$. Thus, the Berry phase for e -particle movement can be calculated even for relatively large system sizes without too much computational cost. The lattice dualities developed in this paper are universal and can be used to study not only the Berry phases of translations of visons, but also many other topological and dynamical properties of these excitations, such as their effective mass and dispersions, which can be crucial in understanding their role in real materials and experiments [31].

ACKNOWLEDGMENTS

C.C. thanks G.-Y. Zhu for enlightening discussions. C.C. and P.R. thank Professor P. Fulde for kind encouragement on pursuing this project. C.C. acknowledges support from the Shuimu Tsinghua Scholar Program.

- [1] X.-G. Wen, *Quantum Field Theory of Many-Body Systems* (Oxford University Press, Oxford, 2010).
- [2] E. Fradkin, *Field Theories of Condensed Matter Physics*, 2nd ed. (Cambridge University Press, Cambridge, UK, 2013).
- [3] P. W. Anderson, The resonating valence bond state in La_2CuO_4 and superconductivity, *Science* **235**, 1196 (1987).

- [4] G. Baskaran, Z. Zou, and P. W. Anderson, The resonating valence bond state and high- T_c superconductivity — a mean field theory, *Solid State Commun.* **63**, 973 (1987).
- [5] N. Read and B. Chakraborty, Statistics of the excitations of the resonating-valence-bond state, *Phys. Rev. B* **40**, 7133 (1989).

- [6] S. Kivelson, Statistics of holons in the quantum hard-core dimer gas, *Phys. Rev. B* **39**, 259 (1989).
- [7] N. Read and S. Sachdev, Large- N Expansion for Frustrated Quantum Antiferromagnets, *Phys. Rev. Lett.* **66**, 1773 (1991).
- [8] T. Senthil and M. P. A. Fisher, Z_2 gauge theory of electron fractionalization in strongly correlated systems, *Phys. Rev. B* **62**, 7850 (2000).
- [9] A. Y. Kitaev, Fault-tolerant quantum computation by anyons, *Ann. Phys. (NY)* **303**, 2 (2003).
- [10] Y.-A. Chen, A. Kapustin, and Đ. Radičević, Exact bosonization in two spatial dimensions and a new class of lattice gauge theories, *Ann. Phys. (NY)* **393**, 234 (2018).
- [11] O. Pozo, P. Rao, C. Chen, and I. Sodemann, Anatomy of Z_2 fluxes in anyon Fermi Liquids and bose condensates, *Phys. Rev. B* **103**, 035145 (2021).
- [12] P. Rao and I. Sodemann, Theory of weak symmetry breaking of translations in Z_2 topologically ordered states and its relation to topological superconductivity from an exact lattice Z_2 charge-flux attachment, *Phys. Rev. Res.* **3**, 023120 (2021).
- [13] A. Kitaev, Anyons in an exactly solved model and beyond, *Ann. Phys. (NY)* **321**, 2 (2006).
- [14] H.-D. Chen and J. Hu, Exact mapping between classical and topological orders in two-dimensional spin systems, *Phys. Rev. B* **76**, 193101 (2007).
- [15] H.-D. Chen and Z. Nussinov, Exact results of the Kitaev model on a hexagonal lattice: Spin states, string and brane correlators, and anyonic excitations, *J. Phys. A: Math. Theor.* **41**, 075001 (2008).
- [16] E. Cobanera, G. Ortiz, and Z. Nussinov, Unified Approach to Quantum and Classical Dualities, *Phys. Rev. Lett.* **104**, 020402 (2010).
- [17] E. Cobanera, G. Ortiz, and Z. Nussinov, The bond-algebraic approach to dualities, *Adv. Phys.* **60**, 679 (2011).
- [18] Z. Nussinov, G. Ortiz, and E. Cobanera, Arbitrary dimensional Majorana dualities and architectures for topological matter, *Phys. Rev. B* **86**, 085415 (2012).
- [19] A. Kapustin and L. Fidkowski, Local commuting projector hamiltonians and the quantum Hall effect, *Commun. Math. Phys.* **373**, 763 (2020).
- [20] Additional details are provided in the Supplemental Material at <http://link.aps.org/supplemental/10.1103/PhysRevResearch.4.043003> file which includes Refs. [12,13,33,34,40,41].
- [21] Here the fact that the statistical interaction only appears when e and m particles are pair fluctuating or hopping along the y direction can be understood as due to the specific “gauge choice” in our duality mapping: each e (m) particle produces a “branch cut” in the vector potential to the right (left) infinity, which is felt by the m (e) particles.
- [22] X.-G. Wen, Quantum orders and symmetric spin liquids, *Phys. Rev. B* **65**, 165113 (2002).
- [23] A. M. Essin and M. Hermele, Classifying fractionalization: Symmetry classification of gapped z_2 spin liquids in two dimensions, *Phys. Rev. B* **87**, 104406 (2013).
- [24] M. Barkeshli, P. Bonderson, M. Cheng, and Z. Wang, Symmetry fractionalization, defects, and gauging of topological phases, *Phys. Rev. B* **100**, 115147 (2019).
- [25] Y.-M. Lu and A. Vishwanath, Classification and properties of symmetry-enriched topological phases: Chern-Simons approach with applications to Z_2 spin liquids, *Phys. Rev. B* **93**, 155121 (2016).
- [26] X.-G. Wen, Quantum Orders in an Exact Soluble Model, *Phys. Rev. Lett.* **90**, 016803 (2003).
- [27] S.-P. Kou, M. Levin, and X.-G. Wen, Mutual Chern-Simons theory for Z_2 topological order, *Phys. Rev. B* **78**, 155134 (2008).
- [28] A. Mesaros and Y. Ran, Classification of symmetry enriched topological phases with exactly solvable models, *Phys. Rev. B* **87**, 155115 (2013).
- [29] S.-P. Kou and X.-G. Wen, Translation-symmetry-protected topological orders in quantum spin systems, *Phys. Rev. B* **80**, 224406 (2009).
- [30] S.-P. Kou and X.-G. Wen, Translation-invariant topological superconductors on a lattice, *Phys. Rev. B* **82**, 144501 (2010).
- [31] A. P. Joy and A. Rosch, Dynamics of visons and thermal Hall effect in perturbed Kitaev models, [arXiv:2109.00250](https://arxiv.org/abs/2109.00250).
- [32] C. Chen and I. Sodemann Villadiego, The nature of visons in the perturbed ferromagnetic and antiferromagnetic Kitaev honeycomb models, [arXiv:2207.09492](https://arxiv.org/abs/2207.09492).
- [33] M. Levin and X.-G. Wen, Fermions, strings, and gauge fields in lattice spin models, *Phys. Rev. B* **67**, 245316 (2003).
- [34] K. Kawagoe and M. Levin, Microscopic definitions of anyon data, *Phys. Rev. B* **101**, 115113 (2020).
- [35] N. Read and D. Green, Paired states of fermions in two dimensions with breaking of parity and time-reversal symmetries and the fractional quantum Hall effect, *Phys. Rev. B* **61**, 10267 (2000).
- [36] M. Sato, Topological odd-parity superconductors, *Phys. Rev. B* **81**, 220504(R) (2010).
- [37] M. Sato and S. Fujimoto, Existence of Majorana Fermions and Topological Order in Nodal Superconductors with Spin-Orbit Interactions in External Magnetic Fields, *Phys. Rev. Lett.* **105**, 217001 (2010).
- [38] M. Geier, P. W. Brouwer, and L. Trifunovic, Symmetry-based indicators for topological Bogoliubov-de Gennes Hamiltonians, *Phys. Rev. B* **101**, 245128 (2020).
- [39] S. Ono, H. C. Po, and H. Watanabe, Refined symmetry indicators for topological superconductors in all space groups, *Sci. Adv.* **6**, eaaz8367 (2020).
- [40] M. Cheng, R. M. Lutchyn, V. Galitski, and S. Das Sarma, Tunneling of anyonic Majorana excitations in topological superconductors, *Phys. Rev. B* **82**, 094504 (2010).
- [41] L. M. Robledo, Sign of the overlap of Hartree-Fock-Bogoliubov wave functions, *Phys. Rev. C* **79**, 021302(R) (2009).